Redox Properties of the Oxo-Bridged Osmium Dimer $[(bpy)_2(OH_2)Os^{III}OOs^{IV}(OH)(bpy)_2]^{4+}$. Implications for the Oxidation of H_2O to O_2

John A. Gilbert, Daniel Geselowitz, and Thomas J. Meyer*

Contribution from the Department of Chemistry, University of North Carolina, Chapel Hill, North Carolina 27514. *Received September 9, 1985*

Abstract: The oxo-bridged Os dimer $[(bpy)_2(H_2O)Os^{III}OOs^{IV}(OH)(bpy)_2]^{4+}$ has been isolated and characterized. Electrochemical experiments in aqueous solution have revealed an extensive redox chemistry for the dimer based on the following couples: Os(V)Os(V)/Os(IV)Os(V), Os(IV)Os(V)/Os(IV)Os(IV), Os(IV)Os(V)/Os(III)Os(IV), Os(IV)Os(IV)/Os(III)Os(IV), Os(III)Os(IV)/Os(III)Os(III), Os(III)Os(III)/Os(II)Os(II). The pH dependences of the potentials for the series of couples are presented and compared to those of the corresponding Ru dimer. The electrochemical results shed considerable light on the role of pH and electronic effects in stabilizing or destabilizing various oxidation states in the thermodynamic sense, in defining decomposition pathways, and in giving insight into the role that the thermodynamic properties of the various oxidation states have in dictating the reactivity properties of the dimers.

When oxidized, the dimer $[(bpy)_2(OH_2)Ru^{III}ORu^{III}(H_2O)(bpy)_2]^{4+}$ provides a basis for the catalytic oxidation of H_2O to O_2[1] and of Cl^- to Cl_2.[2] Characterization of the active form(s) of the dimer and of the mechanism(s) involved in water or Cl^- oxidation are complicated by the reactivity of the oxidized dimer, by the high potentials needed to access its active form or forms, and by its reactivity toward water which is the solvent.

In equivalent coordination environments analogous monomeric polypyridine complex of Os(II) are easier to oxidize than Ru(II) by 0.32–0.60 V.[3-9] The pattern also extends to the higher oxidation state couples involving oxidation states M(VI)/M(V), M(V)/M(IV), and M(IV)/M(III).[10] With the greater ease of oxidation of Os in mind we have turned to the Os analogue of the Ru dimer with two thoughts in mind: (1) The Os dimer could provide a relatively unreactive model for the oxidized, active forms of the Ru dimer. (2) The Ru dimer is a catalyst for the oxidation of water to oxygen, a reaction which it carries out near the thermodynamic potential for the O_2/H_2O couple. If the reactivity characteristics of the Ru dimer are carried over to the Os dimer but at a decreased potential, it is conceivable that the Os dimer could function as a catalyst for the microscopic reverse, the reduction of O_2 to water near the thermodynamic potential for the O_2/H_2O couple.

Experimental Section

Materials. House distilled water was purified by distillation from alkaline permanganate. Solutions of trifluoromethanesulfonic acid, $HOSO_2CF_3$, were prepared from 10-g ampules of the neat acid obtained from Aldrich. Redistilled perchloric acid was obtained from G. F. Smith. Lithium trifluoromethanesulfonate was obtained from Alfa. All other chemicals were reagent grade and were used without further purification.

Preparations. $Os^{II}(bpy)_2Cl_2$. Dichlorobis(bipyridyl)osmium(II) was prepared from $(NH_4)_2Os^{IV}Cl_6$ and 2,2′-bipyridine by a published method.[4]

$[Os^{II}(bpy)_2CO_3]$. (Carbonato)bis(bipyridyl)osmium(II) was prepared according to a literature method[4] with the following modification: argon was constantly bubbled through the reaction mixture during the entire course of the reaction and subsequent crystallization. Failure to rigorously exclude air resulted in impure product.

$[(bpy)_2(OH_2)Os^{III}OOs^{IV}(OH)(bpy)_2](ClO_4)_4\cdot 2H_2O$. $(bpy)_2OsCO_3$ (300 mg) was dissolved in 200 mL of 0.1 M $HClO_4$. After dissolution was complete, the solution was filtered through glass wool. The solution was gently warmed in a beaker to 80–90 °C with stirring. Small aliquots of the solution were removed during the course of the reaction and diluted with 0.1 M $HClO_4$ to monitor the progress of the reaction. After 40 min the visible spectrum showed a minimum amount of $[(bpy)_2Os^{III}(OH_2)(OH)]^{2+}$ (λ_{max} = 370 nm), a maximum amount of the desired product (λ_{max} = 513 nm), and a minimum amount of oxidized product (λ_{max} = 467 nm) and the reaction mixture was cooled on an ice bath. After being cooled at 10 °C for 2 h, the solution was filtered and a solid containing the desired Os^{III}–Os^{IV} dimer and a large amount of impurity was separated by filtration. The volume of the filtrate was reduced by about 20% under vacuum until small crystals of the dimer began to form. After the solution was allowed to sit overnight at room temperature, the microcrystalline product was collected on a medium frit and dried in a desiccator. Yield: 144 mg, 36%. Anal. Calcd: C, 32.24; H, 2.64; N, 7.52. Found: C, 31.93; H, 2.71; N, 7.49.

$[(bpy)_2(OH_2)Os^{III}OOs^{IV}(OH)(bpy)_2](PF_6)_4\cdot H_2O$. The impure solid from the previous preparation was dissolved in 20–30 mL of 0.1 M CF_3SO_3H and potentiostated at +0.55 V vs. SSCE in a two-compartment cell with use of a large platinum screen working electrode, in order to convert all of the dimer present to the Os(III)–Os(IV) form. Two drops of saturated aqueous NH_4PF_6 solution were added and the resulting solid removed by filtration. Four more drops of saturated aqueous NH_4PF_6 were added and the solution was allowed to sit uncovered at room temperature overnight. The resulting solid was collected in a medium frit and recrystallized from warm water. Anal. Calcd: C, 29.04; H, 2.25; N, 6.77. Found: C, 29.08; H, 2.25; N, 6.76.

Instrumentation. UV–vis spectra were recorded on a Bausch and Lomb Model 2000 spectrophotometer. Cyclic and differential pulse voltammetry were performed with use of a Tokai GC-30 glassy carbon disk as the working electrode and the saturated sodium chloride calomel electrode (SSCE) as reference. Rotating disk voltammetry was carried out in three-compartment cells with a Pine Instruments ASR2 rotator. Bulk electrolyses were carried out in a two-compartment cell with either coarse reticulated vitreous carbon or platinum screen working electrodes. Bulk electrolysis/visible spectroscopy experiments were carried out in a three-compartment cell with a 1-cm glass spectrophotometer cell fused onto the working electrode compartment. The cell was fitted with a bubbler tube and a rubber septum for working under inert atmospheres. pH measurements were made with a Radiometer pHM62 meter with electrodes and standard solutions described elsewhere.[1b]

Results

Synthesis. The key intermediate in the preparation of the osmium dimer is $[(bpy)_2Os(OH_2)_2]^{2+}$. Due to the greater inertness toward substitution of Os(II) compared to Ru(II), Ag^+-induced

(1) (a) Gilbert, J. A.; Eggleston, D. S.; Murphy, W. R., Jr.; Geselowitz, D. A.; Gersten, S. W.; Hodgson, D. J.; Meyer, T. J. *J. Am. Chem. Soc.* **1985**, *107*, 3855. (b) Gilbert, J. A. Ph.D. Dissertation, The University of North Carolina, Chapel Hill, NC, 1984. (c) Gersten, S. W.; Samuels, G. J.; Meyer, T. J. *J. Am. Chem. Soc.* **1982**, *104*, 4029. (d) Honda, K.; Frank, A. J. *J. Chem. Soc., Chem. Commun.* **1984**, 1635.

(2) (a) Ellis, C. D.; Gilbert, J. A.; Murphy, W. R., Jr.; Meyer, T. J. *J. Am. Chem. Soc.* **1982**, *104*, 5070. (b) Vining, W.; Meyer, T. J. *J. Electroanal. Chem.* **1985**, *195*, 183; *Inorg. Chem.*, in press.

(3) Kober, D. M.; Sullivan, B. P.; Dressick, W. J.; Caspar, J. V.; Meyer, T. J. *J. Am. Chem. Soc.* **1980**, *102*, 7383.

(4) Kober, E. M. Ph.D. Dissertation, The University of North Carolina, Chapel Hill, NC, 1982.

(5) Sullivan, B. P.; Caspar, J. V.; Johnson, S. R.; Meyer, T. J. *Organometallics* **1984**, *3*, 1241.

(6) Takeuchi, K. J.; Thompson, M. S.; Pipes, D. W.; Meyer, T. J. *Inorg. Chem.* **1984**, *23*, 1845.

(7) Caspar, J. V.; Sullivan, B. P.; Meyer, T. J. *Inorg. Chem.* **1984**, *23*, 2104.

(8) Buckingham, D. A.; Sargeson, A. M. In "Chelating Agents and Metal Chelates"; Academic Press: New York, 1964; pp 237–282.

(9) Buckingham, D. A.; Dwyer, F. P.; Sargerson, A. M. *Inorg. Chem.* **1966**, *5*, 1243.

(10) Takeuchi, K. J.; Samuels, G. J.; Gersten, S. W.; Gilbert, J. A.; Meyer, T. J. *Inorg. Chem.* **1983**, *22*, 1407.

0002-7863/86/1508-1493$01.50/0

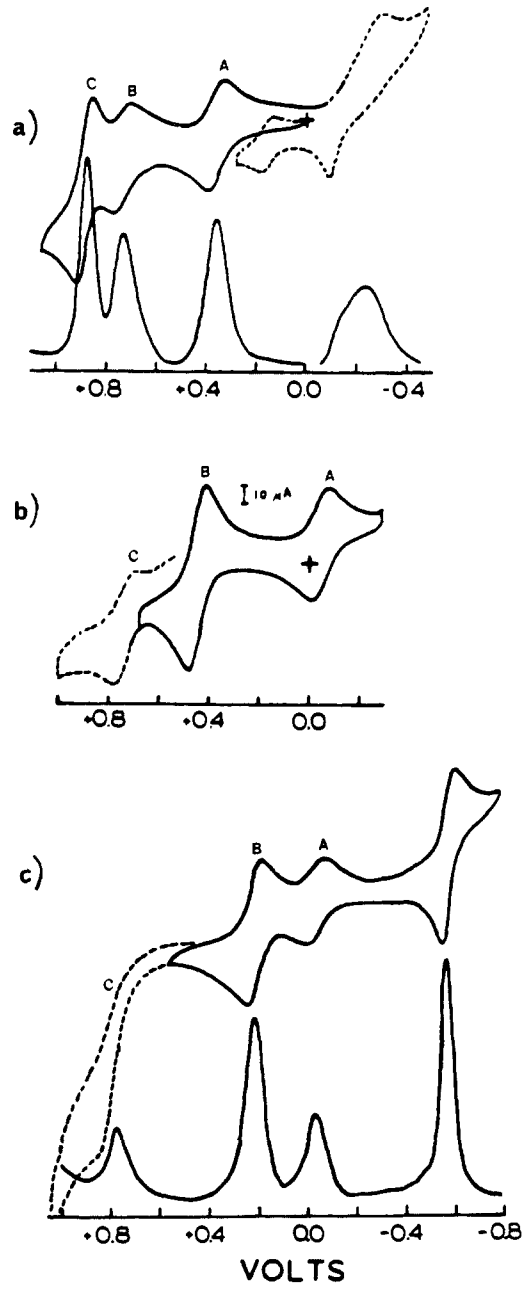

Figure 1. Cyclic (50 mV/s scan rate) and differential pulse voltammograms vs. SCE of $[(bpy)_2(OH_2)OsOOs(OH)(bpy)_2](ClO_4)_4$ in (a) 0.1 M CF_3SO_3H, (b) pH 7.3 phosphate buffer/0.1 M CF_3SO_3Li, and (c) pH 11.0 phosphate buffer at $\mu = 0.1$ M. The concentration of osmium dimer is approximately 0.5 mM.

loss of Cl^- from $(bpy)_2OsCl_2$ was not a synthetically useful route to the diaqua intermediate. Rather, dissolution of $(bpy)_2OsCO_3$ in 0.1 M $HClO_4$ was used to generate the diaqua complex.

$$(bpy)_2OsCO_3 + 2H^+ + H_2O \rightarrow (bpy)_2Os(OH_2)_2^{2+} + CO_2 \quad (1)$$

Spectral observations made during the course of the subsequent heating procedure suggest that dimer formation is preceded by initial oxidation of $[(bpy)_2Os^{II}(OH_2)_2]^{2+}$ to $[(bpy)_2Os^{III}(OH_2)(OH)]^{2+}$ and that at least partial further oxidation to Os(IV) is required for the dimer to form.

Cyclic Voltammetric Oxidation. Cyclic voltammograms of the dimer in water show three waves appearing in the range 0–1 V vs. SSCE and an additional wave below 0 V which is chemically irreversible in acidic solution. As shown in Figure 1 both the pattern of waves and the peak potentials are pH dependent. In acidic solution the pattern of waves above 0 V is a one-electron process interconverting the Os(III)–Os(III) and Os(III)–Os(IV)

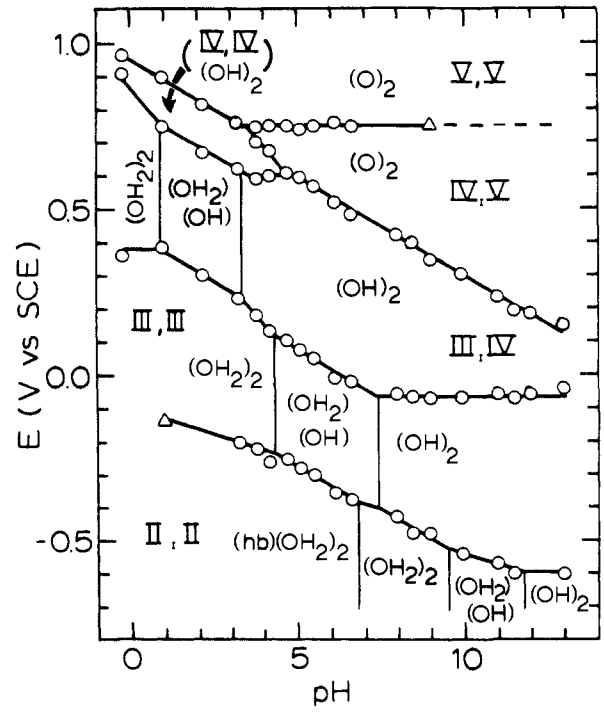

Figure 2. pH dependence of $E_{1/2}$ values vs. SCE measured by cyclic voltammetry for $[(bpy)_2(OH_2)Os^{III}OOs^{IV}(OH)(bpy)_2]^{4+}$. The solid lines depict the theoretical slopes of 0, 28.5, 59, and 118 mV based on the Nernst equation and the pH contents of the various oxidation state forms of the dimers. The vertical lines correspond to pK_a values for the oxidation states shown. The oxidation states at the metal sites in the various pH-potential domains are indicated by Roman numerals. The proton contents inferred from the electrochemical study are indicated by abbreviations like $(OH_2)(OH)$. Thus in the pH–potential domain labeled as III,III-$(OH_2)(OH)$, the dominant form of the dimer is $[(bpy)_2(OH_2)Os^{III}OOs^{III}(OH)(bpy)_2]^{3+}$.

dimers followed by a one- and then a two-electron oxidation. In less acidic solutions the pattern changes to a one- followed by a two- and then a one-electron process. Some of the experimental evidence supporting the electron contents of the processes occurring at the various waves will be presented in due course.

$E_{1/2}$ values for the various couples were determined at a series of pH values. The results are summarized in the $E_{1/2}$–pH or Pourbaix diagram in Figure 2 and the results obtained earlier for the analogous Ru dimer are summarized in Figure 3 for comparison. In these diagrams the vertical lines which occur at the breaks in the $E_{1/2}$–pH curves are pK_a values for the oxidation state entities below the line. Electron and proton contents are also indicated on the diagram in the pH–potential area in which each is the dominant form of the system. The two measurable pK_a values for both the M(III)–M(III) and M(III)–M(IV) dimers estimated from the breaks in the $E_{1/2}$–pH plots or by pH titrations are collected in Table I.

The localized oxidation state descriptions adopted here are a convenience. As noted below, an important feature helping to dictate the redox properties of the dimer may be the existence of strong Os–Os electronic coupling via $d\pi(Os)$–$p\pi(O)$–$d\pi(Os)$ mixing. In some, if not all, of the higher oxidation state cases, the dimers may be electronically delocalized and oxidation state descriptions for the mixed-valence ions like Os(III.5)–Os(III.5) may be more appropriate than Os(III)–Os(IV).

The apparent complexity in the pH–$E_{1/2}$ line for the Os(III)–Os(IV)/Os(III)–Os(III) couple is a consequence of the fact that as the pH is increased from pH 0, pK_a values for the Os(III)–Os(IV) dimer are reached at pH ~1.0 and 3.3 and for the Os(III)–Os(III) dimer at pH 4.3 and 7.3. Above pH 1.0 and 4.3 the dominant forms of the dimers change from diaqua to hydroxo-aqua and above 3.3 and 7.3 to dihydroxo dimers. For those regions in the $E_{1/2}$–pH plot involving $1e^-/0\ H^+$, the slope is 0; for $1e^-/1H^+$ the slope is −59 mV/pH decade, and for $1e^-/2H^+$

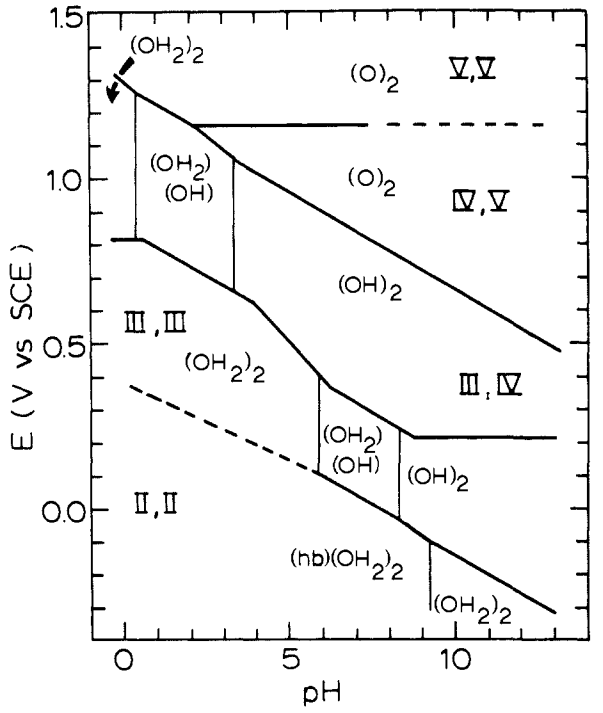

Figure 3. The same diagram as in Figure 2 except for the Ru dimer $[(bpy)_2(OH_2)Ru^{III}ORu^{III}(OH_2)(bpy)_2]^{4+}$. From ref 1a.

Table I. pK_a Values at Room Temperature, μ = 0.1 M

dimer		Ru	Os
$b_2M^{II}(OH)M^{II}b_2^{3+}$ [a]	$pK_{a,hb}$	9.2[b]	5.7[b]
	pK_{a1}	>13	9.5[b]
	pK_{a2}	>13	11.8[b]
$b_2M^{III}OM^{III}b_2^{4+}$	pK_{a1}	5.9[c]	4.3[b]
	pK_{a2}	8.3[c]	7.3[b]
$b_2M^{III}OM^{IV}b_2^{5+}$	pK_{a1}	0.4[d]	1.0[c]
	pK_{a2}	3.2[d]	3.3,[b] 3.5[d]

[a] Proton loss from the μ-hydroxo group. [b] From the breaks in the $E_{1/2}$–pH plots. [c] By pH titration, ±0.2. Reference 1a. [d] By spectrophotometric titration; ±0.2. Reference 1a for the Ru dimer.

the slope is −118 mV/pH decade.

Starting in basic solution for the next higher redox couple, the next oxidation is a $2e^-/2H^+$ process over a broad pH range,

$$20H^- + b_2Os^{III}OOs^{IV}b_2^{2+} \xrightarrow{-2e^-} b_2Os^{IV}OOs^{V}b_2^{3+} + 2H_2O \quad (2)$$

(b is 2,2'-bipyridine)

or past pH 7,

$$b_2Os^{III}OOs^{IV}b_2^{2+} \xrightarrow{-2e^-} b_2Os^{IV}OOs^{V}b_2^{3+} + 2H^+ \quad (2a)$$

The $2e^-$ nature of the couple was verified by coulometry (see below) and the change in proton content follows from the slope of the line. At pH ~5.0 the two-electron couple splits into two, one-electron couples, one pH-independent,

$$b_2Os^{III}OOs^{IV}b_2^{3+} \xrightarrow{-e^-} b_2Os^{IV}OOs^{IV}b_2^{4+} \quad (3)$$

and one involving loss of $2H^+$,

$$b_2Os^{IV}OOs^{IV}b_2^{4+} \xrightarrow{-e^-} b_2Os^{IV}OOs^{V}b_2^{3+} + 2H^+ \quad (4)$$

The $1e^-/2H^+$ couple exists over a narrow pH range since at pH ~3.5 it intersects with the higher oxidation state Os(V)–Os(V)/Os(IV)–Os(V) couple. At pH <3.5 Os(IV)–Os(V) is unstable with respect to disproportionation and the net reaction observed is the $2e^-/2H^+$ oxidation of Os(IV)–Os(IV) to Os(V)–Os(V).

$$b_2Os^{IV}OOs^{IV}b_2^{4+} \xrightarrow{-2e^-} b_2Os^{V}OOs^{V}b_2^{4+} + 2H^+ \quad (5)$$

The pH independence of the Os(III)–Os(IV)/Os(IV)–Os(IV) couple is also restricted to a narrow pH range because of the acid–base properties of Os(III)–Os(IV). At pH ~4.0 the couple becomes

$$b_2Os^{III}OOs^{IV}b_2^{4+} \xrightarrow{-e^-} b_2Os^{IV}OOs^{IV}b_2^{4+} + H^+ \quad (6)$$

and at pH ~1.0,

$$b_2Os^{III}OOs^{IV}b_2^{5+} \xrightarrow{-e^-} b_2Os^{IV}OOs^{IV}B_2^{5+} + 2H^+ \quad (7)$$

Reduction. Cyclic voltammetry and coulometry ($n \sim 2$) below −0.10 V in acidic solutions result in the irreversible, two-electron reductive cleavage of both the Ru and Os dimers,

$$H_2O + 2H^+ + b_2M^{III}OM^{III}b_2^{4+} \xrightarrow{+2e^-} 2b_2M(H_2O)_2^{2+} \quad (8)$$

Following reduction, waves due to the monomers $(bpy)_2M(OH_2)_2^{2+}$ appear as shown in Figure 1a. Above pH 3 for the Os dimer the cleavage reaction is sufficiently slow that as shown in Figure 1c the reduction becomes a chemically reversible 2-electron process.

From the data in Figures 2 and 3 for the M(III)–M(III)/M(II)–M(II) couples, the changes in slope at pH ~5.7 for the Os dimer and at pH ~9.2 for the Ru dimer suggest that the M(II)–M(II) dimers are protonated in more acidic solutions. The protonation presumably occurs at the oxo bridge to give $[(bpy)_2(H_2O)M^{II}(OH)M^{II}(H_2O)(bpy)_2]^{3+}$. For the Ru dimer, in solutions less basic than 9.2, the M(III)–M(III)/M(II)–M(II) couple becomes,

$$3H_2O + b_2Ru^{III}ORu^{III}b_2^{2+} \xrightarrow{+2e^-} b_2Ru^{II}(OH)Ru^{II}b_2^{3+} + 3OH^- \quad (9)$$

until the second pK_a for the Ru(III)–Ru(III) dimer is reached and the couple becomes,

$$2H_2O + b_2M^{III}OM^{III}b_2^{3+} \xrightarrow{+2e^-} b_2M^{II}(OH)M^{II}b_2^{3+} + 2OH^- \quad (10)$$

The greater acidity of Os^{II}–OH_2 monomers compared to Ru^{II}–OH_2[6,10] also appears in the Os(II)–Os(II) dimers. From the breaks in the E vs. pH curve for the Os(III)–Os(III)/Os(II)–Os(II) couple, protons are lost from bound H_2O in successive stages first at pH ~9.5 where the couple becomes,

$$H_2O + b_2M^{III}OM^{III}b_2^{2+} \xrightarrow{+2e^-} b_2M^{II}OM^{II}b_2^{+} + OH^- \quad (11)$$

and then at pH ~11.8 past which the couple is independent of pH.

$$b_2M^{III}OM^{III}b_2^{2+} \xrightarrow{+2e^-} b_2M^{II}OM^{II}b_2 \quad (12)$$

Table II. $E_{1/2}$ Values at pH 7 for the Os and Ru Dimeric Couples vs. SSCE at Room Temperature, μ = 0.1 M (b is 2,2'-bipyridine)

oxidation state couple	$E°'$, V M = Ru	$E°'$, V M = Os
V–V/IV–V		
$b_2(O)M^{V}OM^{V}(O)b_2^{4+}/b_2(O)M^{IV}OM^{V}(O)b_2^{3+}$	1.17	0.76
IV–V/III–IV		
$b_2(O)M^{IV}OM^{V}(O)b_2^{3+}/b_2(OH)M^{III}OM^{IV}(OH)b_2^{3+}$	0.84	0.47
III–IV/III–III		
$b_2(OH)M^{IV}OM^{III}(OH)b_2^{3+}/b_2(OH)M^{III}OM^{III}(H_2O)b_2^{3+}$	0.33	−0.05
III–III/II–II		
$b_2(OH)M^{III}OM^{III}(H_2O)b_2^{3+}/b_2(H_2O)M^{II}(OH)M^{II}(H_2O)b_2^{3+}$	0.05	−0.39

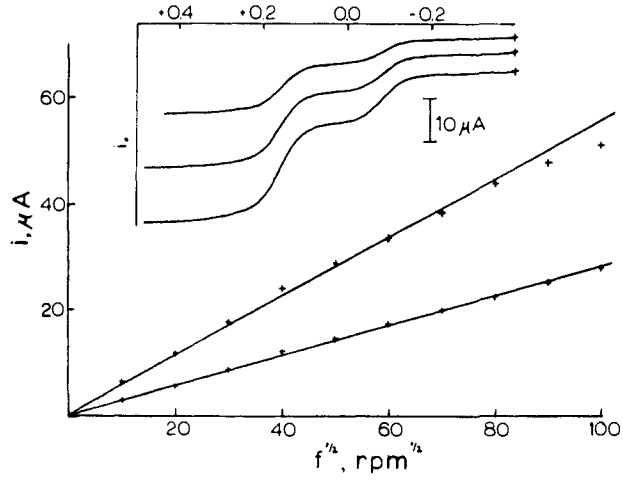

Figure 4. Levich plot constructed from rotated disk voltammograms at pH 11.0 of solutions containing $[(bpy)_2(OH)Os^{III}OOs^{IV}(OH)(bpy)_2]^{3+}$. Curve a: $(i_{+0.025V} - i_{-0.50V})$ vs. $f^{1/2}$. Curve b: $(i_{+0.40V} - i_{0.025V})$ vs. $f^{1/2}$. Inset: Typical voltammograms. [dimer] = 0.503 mM. Supporting electrolyte is the Na_3PO_4/Na_2HPO_4 buffer where $[PO_4^{3-}] + [HPO_4^{2-}] = 0.1$ M.

In Tables I and II are listed comparative pK_a and $E_{1/2}$ values for the Os and Ru dimers and $E_{1/2}$ values for the various redox couples at pH 7.

Coulometry. In order to establish the electron stoichiometries of the redox couples for the Os dimer, bulk electrolyses were carried out at pH 7.34. A solution of 15.5 mg (1.0×10^{-5} mol) of the dimer in 0.1 M NaH_2PO_4/Na_2HPO_4 buffer under argon was first potentiostatted at +0.60 V in order to ensure that all of the sample was present in the Os(III)–Os(IV) form. Reduction at −0.17 V (to Os(III)–Os(III)) occurred with the passage of 1.02 C and reoxidation at +0.20 V by 1.2 C for an average n value of 1.1. Subsequent oxidation of the same solution at +0.54 V to the Os(IV)–Os(V) form occurred with the passage of 2.25 coulombs and rereduction at +0.20 V by 1.8 C for an average n value of 2.1.

Rotating Disk Electrochemistry. A typical disk voltammogram and a Levich plot of i_p vs. $f^{1/2}$ (where f is the electrode rotation rate) are shown in Figure 4. Note that the limiting current for the second oxidation is twice the magnitude of the first oxidation, consistent with the two-electron count observed in coulometry. The diffusion coefficient for the dimer was calculated to be 2.5×10^{-6} cm^2 s^{-1} with use of the slope of the Levich plot for the III–III/III–IV couple and the Levich equation:

$$i_l = 0.62nFAD_0^{2/3}(2\pi f/60)^{1/2}(\upsilon)^{-1/6}(C_0^*)$$

where i_l is the limiting current, n is the number of electrons, F is the Faraday constant, A is the electrode surface area, D_0 is the diffusion coefficient, f is the rotation rate, υ is the kinematic viscosity of the solution, and C_0^* is the concentration of dimer. The line shown in Figure 4 for the second oxidation is calculated by assuming that the second oxidation is a reversible net two-electron process. Although there is deviation of the experimental points from the line at higher rotation rates, the data are consistent with the coulometry data which indicate that the second electrochemical process removes two electrons from the dimer in basic solution.

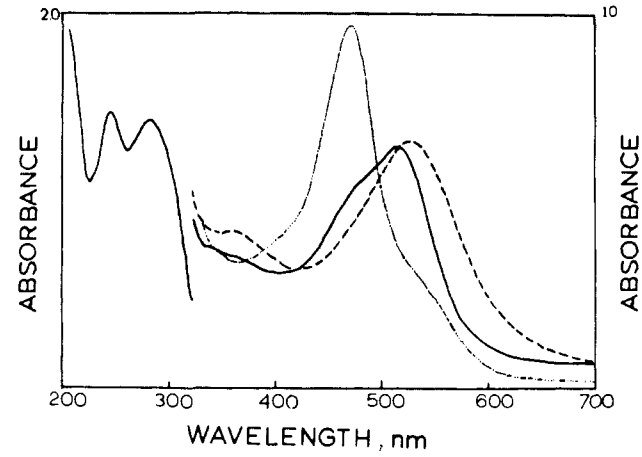

Figure 5. UV–vis spectra of $[(bpy)_2(OH_2)Os^{III}OOs^{IV}(OH)(bpy)_2]^{4+}$ in 0.1 M $HClO_4$ (—), 1.0 M $HClO_4$ (···), and pH 4.5 phosphate buffer (– –). [dimer] = 1.6×10^{-5} M. Cell path length = 1.0 cm.

Plots of log $[i/(i_l - i)]$ vs. E were constructed for both the III–III/III–IV and III–IV/IV–V couples. The slopes of both lines were approximately 59 mV, consistent with one-electron processes.[1b] At first glance, the analysis suggests that the III–IV/IV–V couple may consist of two closely spaced one-electron processes. The limit of resolution of two closely spaced waves by cyclic voltammetry is ~120 mV.[11] From differential pulse voltammetry of the dimer at pH 11 where the III–IV/IV–V couple exhibits its most nearly reversible behavior (Figure 1c), the peak width at half-height is 85 mV. From this value and the ΔE_p value of 55 mV in the cyclic voltammogram the working tables developed by Taube and Richardson[11] suggest that if there are separate waves for the III–IV/IV–IV and IV–IV/IV–V couples they could be separated by as much as 35 mV. However, the Taube–Richardson treatment assumes that both waves are strictly Nernstian at the scan rates employed and the $\Delta E_{1/2}$ value obtained from their working tables must be viewed as an *upper* limit. In fact, the process is probably a 2-electron process, as reported previously for the analogous Ru dimer, perhaps complicated by slow charge-transfer kinetics.

UV–vis Spectra. UV–vis spectra of $(bpy)_2(OH_2)Os^{III}OOs^{IV}(OH)(bpy)_2^{4+}$ are shown in Figure 5 at different pH values. The spectra are qualitatively similar to those obtained for the analogous ruthenium III–IV dimer. The λ_{max} values undergo slight shifts as a function of pH due to the acid–base equilibria discussed previously. In strong acid (1.0 M $HClO_4$) the dominant form of the III–IV dimer is $[(bpy)_2(OH_2)Os^{III}OOs^{IV}(OH_2)(bpy)_2]^{5+}$ and λ_{max} = 470 nm. At pH 2.5 the dominant form of the dimer is $[(bpy)_2(OH_2)Os^{III}OOs^{IV}(OH)(bpy)_2]^{4+}$ and λ_{max} = 518 nm. At pH 5.0 the dominant form is $[(bpy)_2(OH)Os^{III}OOs^{IV}(OH)(bpy)_2]^{3+}$ and λ_{max} = 535 nm. Spectrophotometric determination of the second pK_a value for $[(bpy)_2(OH_2)Os^{III}OOs^{IV}(OH_2)(bpy)_2]^{5+}$ was carried out by diluting aliquots of a stock solution of the III–IV dimer with a variety of phosphate buffers ranging in pH from 3.0 to 5.0. The calculated pK_a value of 3.5 from the spectrophotometric analysis was in good agreement with the value of 3.3 obtained from the Pourbaix diagram in Figure 2.

The spectra of the Os(III)–Os(III) and Os(IV)–Os(IV) dimers in acidic solution (0.1 M CF_3SO_3H) were obtained by using a spectrophotometer cell attached to a three compartment bulk electrolysis cell. The results are shown in Figure 6. In acidic solution, reduction at 0.2 V gave the spectrum of $[(bpy)_2(OH_2)Os^{III}OOs^{III}(OH_2)(bpy)_2]^{4+}$ and oxidation at +0.82 V the spectrum of $[(bpy)_2(OH)Os^{IV}OOs^{IV}(OH)(bpy)_2]^{4+}$. Attempts

(11) Richardson, D. E.; Taube, H. *Inorg. Chem.* **1981**, *20*, 1278.

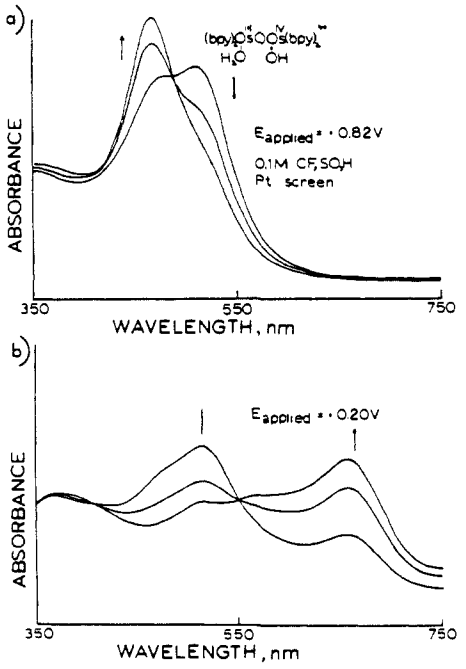

Figure 6. Visible spectra recorded following bulk electrolysis of $[(bpy)_2(OH_2)Os^{III}OOs^{IV}(OH)(bpy)_2]^{4+}$ in 0.1 M CF_3SO_3H at a Pt gauze electrode. (a) Oxidation at +0.82 V to $[(bpy)_2(OH)Os^{IV}OOs^{IV}(OH)(bpy)_2]^{4+}$. (b) Reduction at +0.20 V to $[(bpy)_2(OH_2)Os^{III}OOs^{III}(OH_2)(bpy)_2]^{4+}$.

to generate solutions of the Os(V)–Os(V) form of the dimer electrochemically were unsuccessful. Bulk electrolysis at +1.20 V in 0.1 M CF_3SO_3H resulted in a near complete loss of absorption throughout the visible region. Subsequent rereduction did not result in the reappearance of a lower oxidation state form of the dimer. Comparison of a cyclic voltammogram of the oxidized solution with a solution containing $(phen)Os^{VI}(O)_2(OH)_2$ suggested that the bulk electrolysis product is $(bpy)Os^{VI}(O)_2(OH)_2$ or its conjugate acid $[(bpy)Os^{VI}(O)_2(OH_2)_2]^{2+}$. The Os(V)–Os(V) form of the dimer is apparently stable to loss of bipyridine on the time scale of cyclic voltammetric scans but unstable on the time scale of bulk electrolysis.

The results of reductive bulk electrolysis in 0.1 M NaOH under argon are shown in Figure 7. Reduction at −0.25 V yields $[(bpy)_2(OH)Os^{III}OOs^{III}(OH)(bpy)_2]^{2+}$ which has a series of three broad peaks at λ_{max} = 675, 614, and 440 nm. Further reduction at −0.80 V yields $[(bpy)_2(OH_2)Os^{II}OOs^{II}(OH)(bpy)_2]^{+}$ which shows a similar series of peaks at 540, 480, and 390 nm. Addition of air to solutions of the II–II dimer causes rapid oxidation (within one second) to the III–III form followed by a slower (60 s) oxidation to the III–IV form.

The IV–V form of the dimer could not be generated in strongly basic solution apparently because of catalytic oxidation of a bpy ligand. However, bulk electrolysis of a solution of the Os(II-I)–Os(IV) dimer in pH 8.2 buffer did result in a loss of color coupled with the loss of two electrons as described previously. Repetitive UV–vis scans of a solution of the Os(IV)–Os(V) dimer generated in this manner indicate that reduction back to the Os(III)–Os(IV) dimer occurs over a period of about 15 min. The observations made suggest that the IV–V dimer undergoes a base-catalyzed self-reduction at the metal with concomitant oxidation of a bipyridine ligand or ligands. As discussed later, similar observations have been made in related systems.

Discussion

The Os Dimer. The dimer $[(bpy)_2(OH_2)Os^{III}OOs^{IV}(OH)(bpy)_2]^{4+}$ is one of only eight known osmium dimers bridged by a single oxo group.[1b,12-18] Of the structures that are known the most relevant is $[(tpy)(bpy)Os^{III}OOs^{IV}(bpy)(tpy)](ClO_4)_5$ which has been structurally characterized recently by Roecker.[16] In this dimer, the Os–O–Os bridging angle (170°) and the coplanar pyridyl rings are features shared with the structure of $[(bpy)_2(OH_2)Ru]_2O^{4+}$ reported by Eggleston.[1a,17] Given the structural similarities and the closely related redox chemistries of the diaqua ruthenium and osmium dimers, it is reasonable to conclude that they are probably structurally equivalent. Presumably, the diaqua osmium dimer also contains the slightly bent Os–O–Os group and the coplanar pyridyl rings found in the dimers characterized by Eggleston and Roecker.

Table III. Reduction Potentials for pH-Independent Couples vs. SSCE, μ = 0.1 at Room Temperature

couple	M	$E°'$, V
$b_2(H_2O)M^{III}OM^{IV}(H_2O)b_2^{5+/4+}$	Ru	0.82
	Os	0.48
$b_2(OH)M^{III}OM^{IV}(OH)b_2^{3+/2+}$	Ru	0.21
	Os	0.07
$(trpy)(bpy)M(H_2O)^{3+/2+}$ [a]	Ru	0.79
	Os	0.36
$(trpy)(bpy)M(OH)^{2+/+}$ [a]	Ru	0.32
	Os	0.05

[a] Reference 6.

Oxidation States. A significant feature to emerge from studies on the Ru and Os dimers is the extraordinary richness of their redox chemistries. For example, above pH 7 the Os dimer is accessible in "oxidation states" Os(II)–Os(II), Os(III)–Os(III), Os(III)–Os(IV), Os(IV)–Os(V), and Os(V)–Os(V) to the oxidative and reductive limits of the solvent. Recall that the oxidation state labels used here are a convenience. The actual description of electronic structure in the dimers is potentially complicated by electronic coupling through the bridging oxo group, the extent of which could vary considerably with oxidation state at the metal.

A number of issues arise from the redox studies. They include (1) the basis for the existence of several oxidation states over a relatively narrow potential range, (2) pathways for dimer decomposition, (3) the thermodynamic instability of certain oxidation states and the role that proton content plays in determining oxidation state stability in the thermodynamic sense, (4) comparisons among structurally analogous Fe, Ru, and Os dimers, and (5) the implications that the structural and redox properties of the dimers have for reactivity and catalysis.

Multiple Oxidation States. As for related monomers,[6] the appearance and stabilization of higher oxidation states is tied to the loss of protons. The origin of the effect is electronic and arises because loss of protons from bound H_2O or OH^- leads to the release of π-type electron density at the O atom for donation to the electron deficient, largely metal based $d\pi$ core.

Reductively, the appearance of the M(II)–M(II) dimers is complicated by the 2-electron nature of the III–III → II–II couple and a structural ambiguity. Rather than the diaqua form, $[(bpy)_2(H_2O)M^{II}OM^{II}(H_2O)(bpy)]^{2+}$, the II–II dimers could be based on a di-μ-hydroxo bridge, $[(bpy)_2M^{II}(\mu\text{-}OH)_2M^{II}(bpy)_2]^{2+}$. The chloro-bridged dimer $[(bpy)_2Ru^{II}(\mu\text{-}Cl)_2Ru^{II}(bpy)_2]^{2+}$ is known but is unstable toward bridge splitting in coordinating solvents.[19]

A clear fact that emerges from the Pourbaix diagram in Figure 2 is the profound role that protons play in dictating the redox thermodynamics of the dimers even past the electronic stabilization of higher oxidation states following proton loss. Simple differences

(12) (a) Scroder, M. *Chem. Rev.* **1980**, *80*, 187. (b) Linko, I. V.; Zaitsev, B. E.; Molodkin, A. K.; Ivanova, T. M.; Linko, R. V. *Zh. Neorg. Khim.* **1983**, *28*, 1520.

(13) Armstrong, J. E.; Robinson, W. R.; Walton, R. A. *J. Chem. Soc., Chem. Commun.* **1981**, 1120.

(14) Chakravarty, A. R.; Cotton, F. A.; Schwotzer, W. *Inorg. Chem.* **1984**, *23*, 99.

(15) Tebbe, K. F.; von Schnering, H. G. *Z. Anorg. Allg. Chim.* **1973**, *396*, 66.

(16) Roecker, L.; Hodgson, D. J.; Meyer, T. J., manuscript in preparation.

(17) Eggleston, D. S. Ph.D. Dissertation, The University of North Carolina, Chapel Hill, NC, 1983.

(18) Sugimoto, H.; Higashi, T.; Mori, M.; Nagano, M.; Yoshida, Z.; Ogoshi, H. *Bull. Chem. Soc. Jpn.* **1982**, *55*, 822.

(19) Johnson, E. C.; Sullivan, B. P.; Salmon, D. J.; Adeyemi, S. A.; Meyer, T. J. *Inorg. Chem.* **1978**, *17*, 2211.

in proton content can have a significant impact on redox potentials even for pH-independent couples. For example, from potentials for the $[(bpy)_2(H_2O)M^{III}OM^{IV}(H_2O)(bpy)_2]^{5+/4+}$ and $[(bpy)_2(OH)M^{III}OM^{IV}(OH)(bpy)_2]^{3+/2+}$ couples in Table III, the change in proton content decreases the oxidizing strengths of the III–IV/III–III couples by 0.5–0.6 V. Similar decreases are noted for the related monomeric couples in Table III. The origins of the effect are probably the higher charge types for the aqua couples and electronic stabilization of the higher oxidation state sites by enhanced M–OH or M–O mixing.

The Pourbaix diagrams also summarize in a concise fashion the sometimes remarkable effect that pH variations have on a single couple where a change in proton content occurs between oxidation states. Because oxidation is frequently accompanied by proton loss, the general tendency is for reduction potentials to decrease with an increase in pH. The loss of oxidizing strength is a simple consequence of the proton demands of the couple, e.g.,

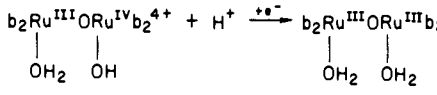

If the dominant form of the reduced part of the couple requires the addition of one or more protons, the oxidizing ability of the oxidized form will necessarily fall as the proton concentration falls. The most complex example of such behavior occurs for the III–IV/III–III couples.

Differences in pH dependences between couples can lead to the thermodynamic stabilization or destabilization of oxidation states. For the Os dimer the IV–IV/III–IV couple appears in acidic solution with the IV–IV dimer existing as $[(bpy)_2(OH)Os^{IV}OOs^{IV}(OH)(bpy)_2]^{4+}$ from pH 0 to ≥4.8. In solutions less acidic than the second pK_a for the III–IV dimer, pH <3.3, the IV–IV/III–IV couple becomes pH independent. The pH independence of the couple assures the demise of Os(IV)–Os(IV) as a thermodynamically stable oxidation state as the pH is raised still further. At pH 4.8 the potentials for the pH-independent IV–IV/III–IV and $2H^+/2e^-$ III–IV/IV–V couple coincide. At pH values higher than 4.8 the Os(IV)–Os(IV) dimer is thermodynamically unstable with respect to disproportionation via

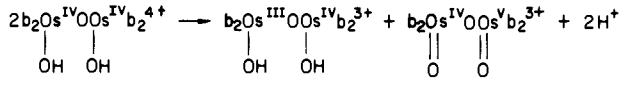

The onset of disporportionation means that in solutions less acidic than pH 4.8, the IV–IV dimer is a stronger oxidant than the IV–V dimer. The reversal in expected oxidizing strength is a simple consequence of the proton demands associated with the IV–V/IV–IV couple,

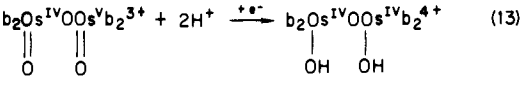

(13)

which drop its potential below the potential for the IV–IV/III–IV couple,

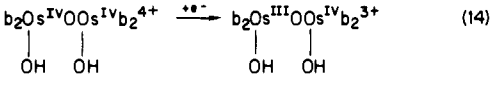

(14)

as the solution becomes less acidic.

In acidic solution the Os(IV)–Os(V) dimer suffers the same fate as the Os(IV)–Os(IV) dimer. From the Pourbaix diagram, at pH <4.8 the $2e^-/2H^+$ IV–V/III–IV couple splits into the $1e^-$-III–IV/IV–IV and the $1e^-/2H^+$-IV–IV/IV–V couples shown in eq 13 and 14. This state of affairs is temporary since by pH 3.7 the pH-dependent IV–IV/IV–V couple intersects the pH-independent IV–V/V–V couple. In solutions more acidic, the Os(IV)–Os(V) dimer is unstable with respect to disproportionation,

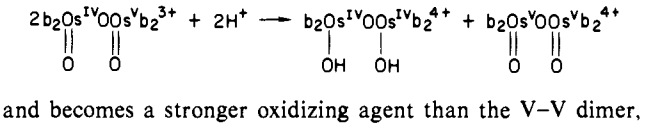

and becomes a stronger oxidizing agent than the V–V dimer,

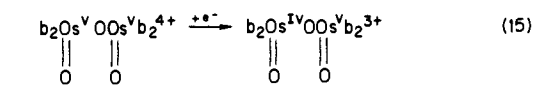

(15)

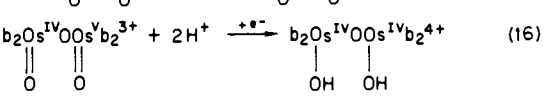

(16)

because of the effect of the increase in proton concentration on the potential of the IV–V/IV–IV couple.

Given the $1e^-/2H^+$ character of the III–IV/IV–IV couple in strongly acidic solution,

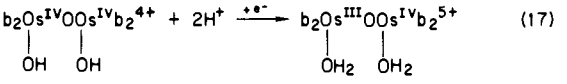

(17)

and the $2e^-/2H^+$ character of the IV–IV/V–V couple, at a higher, experimentally unobtainable, acidity the III–IV/IV–IV couple would cross the IV–IV/V–V couple. Past that point, Os(IV)–Os(IV) would become unstable with respect to disproportionation,

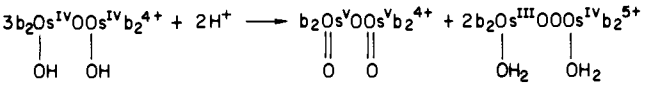

and also a stronger oxidizing agent than the V–V dimer,

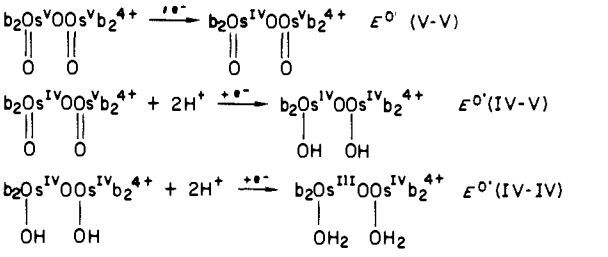

In strongly acidic solution the extrapolated order of the reduction potentials for the three couples above would become $E^{\circ\prime}$(IV–V) > $E^{\circ\prime}$(IV–IV) > $E^{\circ\prime}$(V–V).

The extrapolated behavior for the Os dimer helps to explain the experimentally observed behavior for the Ru dimer in acidic solution. From the Pourbaix diagrams in Figures 2 and 3, a key difference between the Ru and Os dimers is that oxidation state Ru(IV)–Ru(IV) must be relatively destabilized and the potential for the pH-independent III–IV/IV–IV couple,

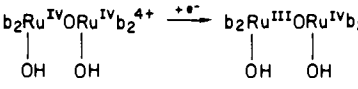

must actually lie above the potential for the IV–V/V–V couple,

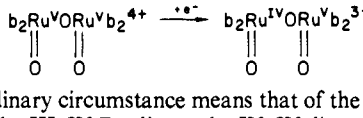

This extraordinary circumstance means that of the three oxidation states above the III–IV Ru dimer, the IV–IV dimer is the strongest oxidizing agent and the order of reduction potentials is $E^{\circ\prime}$(IV–IV) > $E^{\circ\prime}$(IV–V) > $E^{\circ\prime}$(V–V).

As for the Os dimer, the III–IV/IV–V couple is a $2e^-/2H^+$ couple over a broad pH range,

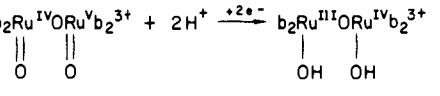

However, at pH <2.3 the potential for the III–IV/IV–V couple crosses the pH-independent IV–V/V–V couple and the IV–V dimer becomes unstable with respect to disproportionation,

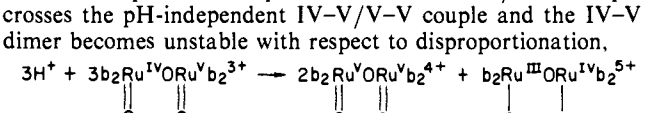

In this region the experimentally observed couple is $3e^-/3H^+$ in nature,

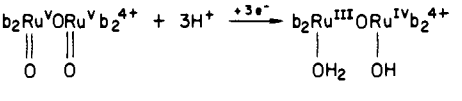

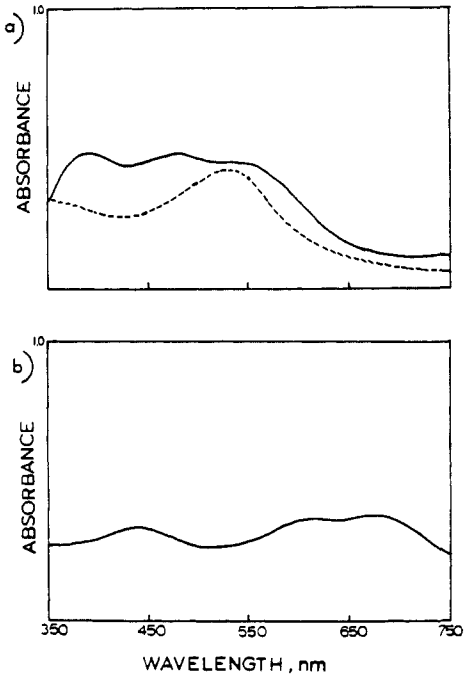

Figure 7. Visible spectra of (a) electrochemically generated $[(bpy)_2(OH)Os^{II}OOs^{II}(OH_2)(bpy)_2]^+$ in 0.1 M NaOH under argon (—) and after exposure to air to give $[(bpy)_2(OH)Os^{III}OOs^{IV}(OH)(bpy)_2]^{3+}$ (– –) and (b) electrochemically generated $[(bpy)_2(OH)Os^{III}OOs^{III}(OH)(bpy)_2]^{2+}$ in 0.1 M NaOH. [dimer] = 6×10^{-5} M. Cell path length = 1.0 cm.

until pH 0.4 where the first pK_a for Ru(III)–Ru(IV) is reached and the couple becomes $3e^-/4H^+$ in nature,

$$b_2Ru^{V}(O)ORu^{V}(O)b_2^{4+} + 4H^+ \xrightarrow{+3e^-} b_2Ru^{III}(OH_2)ORu^{IV}(OH_2)b_2^{5+}$$

In pursuing the theme of "missing" oxidation states there are two additional points to be made. The first is also acid–base related. If the first pK_a for oxo formation for the Os(IV)–Os(IV) dimer had occurred before the intersection between the IV–IV/III–IV and IV–V/III–IV couples at pH 4.8, the one-electron IV–IV/III–IV and IV–V/IV–IV couples,

$$b_2Os^{V}(O)OOs^{V}(O)b_2^{4+} + H^+ \xrightarrow{+e^-} b_2Os^{IV}(OH)OOs^{IV}(O)b_2^{4+}$$

$$b_2Os^{IV}(OH)OOs^{IV}(O)b_2^{4+} + H^+ \xrightarrow{+e^-} b_2Os^{III}(OH)OOs^{IV}(OH)b_2^{4+}$$

would be experimentally observable and Os(IV)–Os(IV) stable over a broader pH range. The disappearance of Os(IV)–Os(IV) as a stable oxidation state past pH 4.8 is a direct consequence of the fact that the Os^{IV}–OH protons are not appreciably acidic in the dimer.

The second point is to the possible role of electronic effects in the nonappearance of the oxidation state M(II)–M(III). Over the experimentally accessible pH range the III–III → II–II reduction is a 2-electron process. This necessarily means that potentials for the sequential $1e^-/1H^+$ reductions from pH 5.8 to 9.5,

$$b_2M^{III}(OH)OM^{III}(OH)b_2^{2+} + H^+ \xrightarrow{+e^-} b_2M^{II}(OH_2)OM^{III}(OH)b_2^{2+}$$

$$b_2M^{II}(OH_2)OM^{III}(OH)b_2^{2+} + H^+ \xrightarrow{+e^-} b_2M^{II}(OH_2)OM^{II}(OH_2)b_2^{2+}$$

are arranged so that the II–III dimer is a stronger oxidant than the III–III dimer. Thus the II–III dimer is unstable with respect to disproportionation,

$$2b_2M^{II}(OH_2)OM^{III}(OH)b_2^{2+} \longrightarrow b_2M^{II}(OH_2)OM^{II}(OH_2)b_2^{2+} + b_2M^{III}(OH)OM^{III}(OH)b_2^{2+}$$

In this case there is no net proton gain or loss and since products and reactants are of the same charge type, differences in solvation free energies should play a relatively minor role in dictating relative stabilities. Although a special stability is normally associated with "mixed-valence" ions, this is a case where the "mixed-valence" ion, $[(bpy)_2(H_2O)M^{II}OM^{III}(OH)(bpy)_2]^{2+}$, is unstable with regard to the adjacent oxidation states. The origin of the instability must lie in electronic effects, a detailed analysis of which is not a goal of this paper. However, on the basis of a qualitative molecular orbital analysis for the dimer $[(bpy)_2ClRu^{III}ORu^{III}Cl(bpy)_2]^{2+}$, the fact that the ground state is a magnetic spin triplet can be explained by the occupation of two degenerate or nearly degenerate levels, π_1^* and π_2^*, which are antibonding with respect to the Ru–O–Ru bridge and largely $d\pi$(Ru) in character.[20] Assuming that the same MO scheme also applies to the II–III and II–II dimers, reduction past the III–III stage involves sequential addition of electrons to π^*_1, and π_2^*

$$\text{III–III}(\pi_1^*)^1(\pi_2^*)^1 \xrightarrow{+e^-} \text{II–III}(\pi_1^*)^2(\pi_2^*)^1 \xrightarrow{+e^-} \text{II–II}(\pi_1^*)^2(\pi_2^*)^2$$

One contributing factor to the electronic instability of the mixed-valence ion may be the presence of an additional electron in the Ru–O–Ru π^* orbitals.

A similar situation must also exist for the sequential $1e^-/1H^+$ reductions of Os(IV)–Os(V),

$$b_2Os^{IV}(O)OOs^{V}(O)b_2^{3+} + H^+ \xrightarrow{+e^-} b_2Os^{IV}(OH)\text{-}Os^{IV}(O)b_2^{3+}$$

$$b_2Os^{IV}(OH)OOs^{IV}(O)b_2^{3+} + H^+ \xrightarrow{+e^-} b_2Os^{III}(OH)OOs^{IV}(OH)b_2^{3+}$$

In this case the fact that the one-electron couples are not observed shows that the intermediate oxidation state, Os(IV)–Os(IV), is unstable with respect to disproportionation into the adjacent mixed-valence dimers,

$$2b_2Os^{IV}(OH)OOs^{IV}(O)b_2^{3+} \longrightarrow b_2Os^{IV}(O)OOs^{V}(O)b_2^{3+} + b_2Os^{III}(OH)OOs^{IV}(OH)b_2^{3+}$$

Decomposition Pathways. Although the Os dimer exists in a plethora of oxidation states, there are three discrete decomposition pathways accessible which limit stability at the high and low ends of the oxidation state range. Reduction to M(II)–M(II) results in hydrolysis and cleavage of the dimer,

$$b_2M^{II}(OH_2)OM^{II}(OH_2)b_2^{2+} + H_2O + 2H^+ \longrightarrow 2b_2M^{II}(H_2O)_2^{2+}$$

which is greatly accelerated as pH is decreased. By pH 3 for the Os dimer and pH 5 for the Ru dimer, the breakdown of the dimer is sufficiently rapid that the III–III → II–II reduction is chemically irreversible at scan rates of 200 mV/s.

For the highest oxidation state, Os(V)–Os(V), in acidic solution there is also a limited stability, in this case, on time scales longer than cyclic voltammetry. The decomposition involves loss of bpy, breakdown of the dimer, and oxidation to Os(VI),

$$b_2Os^{V}(O)OOs^{V}(O)b_2^{4+} + 5H_2O \xrightarrow{-2e^-} 2(bpy)Os^{VI}(O)_2(OH)_2 + 2bpyH^+ + 4H^+$$

The tendency to lose polypyridine ligands following oxidation to Os(V) or Os(VI) appears to be general on the basis of studies of monomeric complexes,

(20) Weaver, T. R.; Meyer, T. J.; Adeyemi, S. A.; Brown, G. M.; Eckberg, R. P.; Hatfield, W. E.; Johnson, E. C.; Murray, R. W.; Untereker, D. *J. Am. Chem. Soc.* **1975**, *97*, 3039.

$$2H_2O + (trpy)(bpy)Os^{V}O^{2+} \xrightarrow{-e^-} (trpy)Os^{VI}(O)_2OH + bpyH^+ + 2H^+ \quad 6$$

$$2H_2O + cis\text{-}(bpy)_2Os^{VI}(O)_2^{2+} \rightarrow (bpy)Os^{VI}(O)_2(OH)_2 + bpyH^+ + H^+ \quad 21$$

The key feature driving ligand loss appears to be the electronic stabilization associated with formation of the trans-dioxo structure at Os(VI), e.g.,

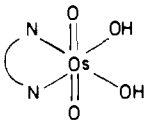

At pH 8, solutions containing the Os(IV)–Os(V) dimer can be generated by coulometric oxidation of the III–III dimer. However, even the IV–V dimer is unstable on the time scale of several minutes. It appears to return quantitatively to the III–IV dimer based on spectrophotometric studies. The rate of decomposition is greatly enhanced in more strongly basic solutions. The experimental observations made here exactly parallel those made earlier on the decomposition of $Ru(bpy)_3^{3+}$[22,23] and of oxo complexes like $[(trpy)(bpy)Ru{=}O]^{2+}$[24] in basic solution. The decomposition chemistry occurring is base-induced oxidative degradation of the polypyridine ligands through initial steps like

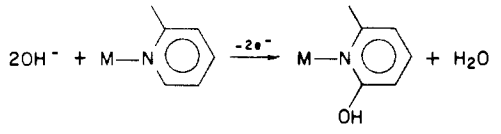

The ligand can be further oxidized and the steps past the first are greatly accelerated ratewise. When carried over to the IV–V dimer, in the net sense, the IV–V → III–IV conversion must occur accompanied by the appearance of a minor part of the III–IV product which contains a multiply oxidized bpy ligand or ligands.

Comparison of Redox Properties Among Structurally Equivalent Fe, Ru, and Os Dimers. The preparation and characterization of the Os dimer completes the sequence of dimers $[(bpy)_2(H_2O)M^{III}OM^{III}(H_2O)(bpy)_2]^{4+}$ (M = Fe, Ru, Os). The results of X-ray crystallographic studies show that the structures of the Fe[25] and Ru[1a] dimers are closely related with bent M–O–M bridges and *cis*-bpy configurations at the metal, and it was concluded above that the structure of the Os dimer is very likely similar.

Given the similarity in structures, the difference in redox properties between Fe on one hand and Ru and Os on the other is striking. In order to illustrate the differences, a series of reduction potentials are collected in Table IV.

The order of reduction potentials for the $M(bpy)_3^{3+/2+}$ couples, Ru > Fe > Os, can be largely understood on the basis of the order of the third ionization energies of the metals and such effects as $d\pi \rightarrow \pi^*$(bpy) back-bonding in oxidation state M(II).[26] Although the order Ru > Os is maintained in the III–IV/III–III couples, no evidence for oxidation of the Fe dimer past Fe(III)–Fe(III) was found to the solvent limit at either pH 1.0 or 6.0.

In the dimers, Fe(IV) is destablized oxidatively relative to Ru(IV) by >0.6 V whereas in the $M(bpy)_3^{3+/2+}$ monomers Fe(III) is stabilized relative to Ru(III) by 0.2 V. An important factor may be the much smaller $3d\pi$ orbital extension for Fe compared to $4d\pi$ or $5d\pi$ for Ru or Os. From the discussion above an important feature in the electronic structures of the Ru(III) and Os(III) dimers appears to be strong $d\pi$–$p\pi$(O)–$d\pi$ mixing. Electrons are lost from antibonding levels

$$(\pi_1^*)^1(\pi_2^*)^1 \xrightarrow{-e^-} (\pi_1^*)^0(\pi_2^*)^1$$

Although magnetic exchange exists between the Fe(III) sites in the Fe dimer,[25,27] there is no evidence for strong electronic coupling. Oxidation past Fe(III) to Fe(IV) may involve loss of electrons from levels which are, to a much greater extent, $d\pi$ Fe(III) in character. In addition, for oxidation states Ru(IV) or Os(IV) in the dimers or in monomers like $[(trpy)(bpy)M(O)]^{2+}$ additional electronic stabilization at the electron-deficient metal sites arises from proton loss and metal oxo formation based on $p\pi(O) \rightarrow d\pi(M)$ donation and mixing. The degree of stabilization for Fe(IV) from this source must be far less than that for Ru and Os as evidenced, for example, by the absence of a wave up to 1.1 V at pH 6 for an $Fe^{IV}{=}O$ couple like

$$[(bpy)_2(OH)Fe^{III}OFe^{III}(OH)(bpy)_2]^{2+} \xrightarrow{-e^-} [(bpy)_2(O)Fe^{IV}OFe^{III}(OH)(bpy)_2]^{2+} + H^+$$

The order Ru > Os is maintained through monomeric and dimeric couples involving higher oxidation states. The exception is in the relative destabilization of the Ru(IV)–Ru(IV) dimer compared to Os(IV)–Os(IV). The fact that the higher oxidation states of Os and Ru are stabilized relatively equally in the dimers may arise because of the nature of the M–O electronic interactions both across the oxo bridge and between the individual metal sites at the terminal oxo groups. An important component in the M–O interaction is $d\pi$(M)–$p\pi$(O) mixing. The extent of $d\pi$–$p\pi$ mixing is greater for Os by virtue of the greater radial extent of 5d vs. 4d orbitals. However, $d\pi$–$p\pi$ mixing is favored for Ru on orbital energy grounds. Ru is intrinsically more electron deficient and the metal-based $4d\pi$ orbitals are nearer $p\pi$(O) in energy which increases the extent of interaction.

Implications for Redox Reactivity. The subtle and sometimes intricate pattern of redox couples uncovered in the electrochemical study has some clear implications for the reactivity properties of the dimers toward oxidation and reduction. The importance of pH and proton content in dictating thermodynamic properties has been well documented here. Proton content can also play a role in dictating which of several possible mechanistic pathways will be of lowest energy. This has proven to be the case for Ru(IV) monomers like $[(bpy)_2(py)Ru^{IV}{=}O]^{2+}$ where in order to avoid simple one-electron transfer to give reduced forms which are proton deficient

$$b_2(py)Ru^{IV}O^{2+} \xrightarrow{+e^-} b_2(py)Ru^{III}O^+$$

more complex pathways appear[28] involving H atom,[29] hydride ion,[30] or O atom[31] transfers. Much the same behavior can be anticipated for dimeric couples which involve net changes in proton content, e.g.,

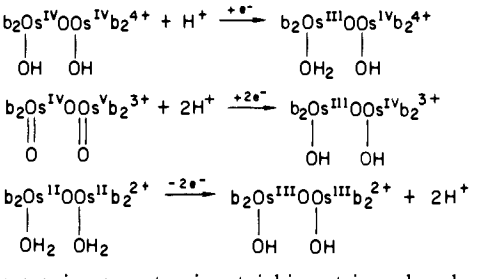

perhaps presaging an extensive stoichiometric and perhaps elec-

(21) Dobson, J.; Meyer, T. J., submitted.
(22) Ghosh, P. K.; Brunschwig, B. S.; Chou, M.; Creutz, C.; Sutin, N. *J. Am. Chem. Soc.* **1984**, *106*, 4772.
(23) Nord, G.; Pedersen, B.; Bjergbakke, E. *J. Am. Chem. Soc.* **1983**, *105*, 1913.
(24) Roecker, L.; Kutner, W.; Gilbert, J. A.; Simmons, M.; Murray, R. W.; Meyer, T. J. *Inorg. Chem.* **1985**, *24*, 3784.
(25) Plowman, J. E.; Loehr, T. M.; Schauer, C. K.; Anderson, O. P. *Inorg. Chem.* **1984**, *23*, 3553.
(26) Buckingham, D. A.; Sargeson, A. M. In "Chelating Agents and Metal Chelates"; Dwyer, F. P., Mellor, D. P., Eds.; Academic Press, NY, 1964; pp 231–280.
(27) Khedekar, A. V.; Lewis, J.; Mabbs, F. E.; Weigold, H. *J. Chem. Soc. A* **1967**, 1561.
(28) Meyer, T. J. *J. Electrochem. Soc.* **1984**, *131*, 7, 221C–228C.
(29) (a) Binstead, R. A.; Moyer, B. A.; Samuels, G. J.; Meyer, T. J. *J. Am. Chem. Soc.* **1981**, *103*, 2897–2899. (b) Roecker, L.; Meyer, T. J., manuscript in preparation.
(30) (a) Thompson, M. S.; Meyer, T. J. *J. Am. Chem. Soc.* **1982**, *104*, 4106. (b) Thompson, M. S.; Meyer, T. J. *J. Am. Chem. Soc.* **1982**, *104*, 5070. (c) Roecker, L.; Meyer, T. J. *J. Am. Chem. Soc.*, in press.
(31) (a) Moyer, B. A.; Sipe, B. K.; Meyer, T. J. *Inorg. Chem.* **1981**, *20*, 1475. (b) Moyer, B. A.; Meyer, T. J. *J. Am. Chem. Soc.* **1979**, *101*, 1326.

Table IV. Reduction Potential Comparisons Amongst Analogous Complexes of Fe, Ru, and Os vs. SSCE, μ = 0.1 M at Room Temperature

couple	$E^{\circ\prime}$, V Fe	Ru	Os
$M^{III}(bpy)_3^{3+}/M^{II}(bpy)_3^{2+}$	1.10	1.30	0.88
$b_2M^{III}OM^{IV}b_2^{4+}/b_2M^{III}OM^{III}b_2^{4+}$ (at pH 1)	>1.4	0.79	0.48
$b_2M^{III}OM^{IV}b_2^{3+}/b_2M^{III}OM^{III}b_2^{3+}$ (at pH 6)	>1.1	0.40	0.02
$(trpy)(bpy)M^{IV}(O)^{2+}/(trpy)(bpy)M^{III}(OH)^{2+}$ (at pH 6)		0.62	0.47

trocatalytic redox chemistry based on complex mechanistic pathways.

The appearance of net two- or even three-electron couples because of the thermodynamic instability of intermediate oxidation states immediately raises the possibility of introducing multiple electron, hydride, or O atom transfers. The special features of multiple electron couples may also influence electrode reactions or chemical reactions where the other reactant is restricted to 1-electron transfers. Restriction of a 2-electron couple to electron transfer via successive 1-electron steps means that the first step necessarily involves a high-energy intermediate, e.g.,

$$b_2Os^{III}OOs^{IV}b_2^{3+} \xrightarrow{-e^-} b_2Os^{IV}OOs^{IV}b_2^{4+}$$

followed by the thermodynamically more favored oxidation (or reduction) of the intermediate oxidation state,

$$b_2Os^{IV}OOs^{IV}b_2^{4+} \xrightarrow{-e^-} b_2Os^{IV}OOs^{V}b_2^{3+} + 2H^+$$

If the difference in potentials between the initial one-electron step and the overall two-electron couple,

$$b_2Os^{III}OOs^{IV}b_2^{3+} \xrightarrow{-2e^-} b_2Os^{IV}OOs^{V}b_2^{3+} + 2H^+$$

becomes too great, slow electron transfer and electrochemical irreversibility could result. Such effects could help explain why, for example, the IV–V/III–IV couple for the Ru dimer becomes noticeably irreversible in solutions of intermediate pH where the intermediate oxidation state Ru(IV)–Ru(IV) is thermodynamically unstable.

The thermodynamic instability of Ru(IV)–Ru(IV) may also play a role in the activity of the Ru dimer as a catalyst toward the oxidation of water to O_2. In an earlier paper the point was made that oxidation states Ru(V)–Ru(V) and Ru(IV)–Ru(V) (and by inference Ru(IV)–Ru(IV)) are all thermodynamically capable of oxidizing water to O_2.[1a] However, the V–V dimer is distinctive in having the requisite four-electron capability within a single chemical site,

$$b_2Ru^{V}ORu^{V}b_2^{4+} + 2H_2O \longrightarrow b_2Ru^{III}ORu^{III}b_2^{4+} + O_2 \quad (18)$$

and may, in fact, be the active form of the catalyst. However, because of the thermodynamic instability of Ru(IV)–Ru(IV), in acidic solution a single 1-electron oxidation past the Ru(III)–Ru(IV) stage is adequate to reach Ru(V)Ru(V) and achieve water oxidation. The sequence of events would, of course, involve initial 1-electron oxidation,

$$b_2Ru^{III}ORu^{IV}b_2^{5+} \xrightarrow{-e^-} b_2Ru^{IV}ORu^{IV}b_2^{4+} + 2H^+$$

followed by disproportionation to give Ru(V)–Ru(V),

$$2H^+ + 3b_2Ru^{IV}ORu^{IV}b_2^{4+} \longrightarrow b_2Ru^{V}ORu^{V}b_2^{4+} + 2b_2Ru^{III}ORu^{IV}b_2^{5+}$$

Once reached by 2-electron oxidation, Ru(IV)Ru(V) would also undergo disproportionation to reach Ru(V)Ru(V),

$$4H^+ + 3b_2Ru^{IV}ORu^{V}b_2^{3+} \longrightarrow 2b_2Ru^{V}ORu^{V}b_2^{4+} + b_2Ru^{III}ORu^{IV}b_2^{5+}$$

In acidic solution the pattern of redox couples exhibited by the Ru dimer is nearly ideal for minimizing the "overvoltage" to H_2O oxidation for the dimer acting as an electrocatalyst. The key is the existence of the 3e$^-$, III–IV → V–V couple which at pH 1 is 300 mV above the potential for the O_2/H_2O couple. The potential for the 4-electron V–V/III–III couple is determined by the weighted sum of the potentials for the 3-electron and 1-electron couples. The 3-electron V–V/III–IV couple is sufficiently oxidizing that water oxidation via the 4-electron couple in eq 18 is spontaneous by $E^{\circ\prime}$ = 0.21 V at pH 1. As an electrocatalyst the "chemical overvoltage" for the Ru dimer is necessarily fixed by the potential of the 3-electron III–IV → V–V oxidation since the V–V dimer must be reached before oxidation can occur. The overvoltage for H_2O oxidation is low because of the close proximity of the O_2/H_2O and V–V/III–IV couples.

The Os dimer has the same pattern of redox couplex, but the pattern that minimizes overvoltage for water oxidation by the Ru dimer ensures that, as an electrocatalyst for $O_2 \rightarrow H_2O$, the Os dimer must necessarily operate with a higher overvoltage. For the oxidation of $[(bpy)_2(OH_2)Os^{III}OOs^{III}(OH_2)(bpy)_2]^{4+}$ by O_2,

$$b_2(OH_2)Os^{III}OOs^{III}(OH_2)b_2^{4+} + O_2 \rightarrow b_2(O)Os^{V}OOs^{V}(O)b_2^{4+} + 2H_2O \quad (19)$$

$E^{\circ\prime}$ = 0.44 V at pH 1.0.

In fact, the Os(III)–Os(III) dimer *is* oxidized by atmospheric O_2 to Os(III)–Os(IV). The mechanistic details of the reaction are as yet unstudied and may simply involve initial one-electron transfer via

$$b_2Os^{III}OOs^{III}b_2^{4+} + O_2 \longrightarrow b_2Os^{III}OOs^{IV}b_2^{5+} + O_2^-$$

They may also involve the microscopic reverse of water oxidation by the Ru dimer utilizing a complex multielectron step

$$b_2Os^{III}OOs^{III}b_2^{4+} + O_2 \longrightarrow b_2Os^{V}OOs^{V}b_2^{4+} + 2H_2O \quad (?)$$

followed by comproportionation between Os(V)–Os(V) and Os(III)–Os(III) to give Os(III)–Os(IV)

$$4H^+ + b_2Os^{V}OOs^{V}b_2^{4+} + 3b_2Os^{III}OOs^{III}b_2^{4+} \longrightarrow 4b_2Os^{III}OOs^{IV}b_2^{5+}$$

Regardless of the detailed mechanism for O_2 activation, and even if the 4-electron step is operative, electrochemical regeneration of the reductively active III–III form of the dimer

$$b_2Os^{III}OOs^{IV}b_2^{4+} + H^+ \xrightarrow{+e^-} b_2Os^{III}OOs^{III}b_2^{4+}$$

requires the application of a potential past the III–IV/III–III couple at 0.73 V (vs. NHE; 0.48 V vs. SCE) at pH 1. Since the O_2/H_2O potential at pH 1 is 1.17 V vs. NHE, this necessarily creates a higher overvoltage for O_2 reduction by the Os dimer than the 0.21 V overvoltage for H_2O oxidation by the Ru dimer.

Acknowledgments are made to the National Institutes of Health under grant No. 5-RO1-GM32296-03 for support of this research.